TOWARDS ROBUST DESIGN OF CLOSED-LOOP NONLINEAR SYSTEMS WITH INPUT AND STATE CONSTRAINTS

Johannes Gerhard, Wolfgang Marquardt, Martin Mönnigmann

Lehrstuhl für Prozesstechnik, RWTH Aachen University
Turmstr. 46, D-52064 Aachen, Germany

Abstract: In this paper we address the task of finding a robust process and control design for nonlinear systems with uncertainties and disturbances such that bounds on inputs and outputs are not violated. The solution of this task is approached by Constructive Nonlinear Dynamics (CNLD), an optimization based method developed by the authors in recent years. CNLD guarantees robustness by backing off a nominal point of operation from critical manifolds. Critical manifolds are boundaries in the space of system and controller parameters that separate regions with qualitatively different system behavior, such as a region with stable operating points from a region with unstable system behavior. In this work, CNLD is adopted and extended to account for bounds and constraints on trajectories of inputs and states. Critical boundaries in the parameter space are presented that separate a region where all trajectories stay within the bounds from a region where trajectories violate the constraints. Constraints ensuring a minimal back off from this new type of critical manifold are derived. Application to an illustrative case study demonstrates the feasibility of the approach. *Copyright © 2006 IFAC*

Keywords: robust nonlinear control, disturbances, constraints

1. INTRODUCTION

In most process systems, bounds on inputs and states must not be violated for safety reasons or because of product specifications even in the presence of process uncertainties and disturbances. A large number of articles addresses the task of process and control design to guarantee that constraints on inputs and outputs hold in the presence of disturbances. Nonlinear model predictive control is widely used for systems with constraints, including robust control with min-max formulations in the presence of uncertainties, see e.g. the survey paper (Mayne *et al.*, 2000). Other approaches that address constrained robust nonlinear control include Lyapunov based techniques (El-Farra and Christofides, 2001) or the combination of feedback linearizing control and linear model predictive control (Kurtz and Henson, 1997).

In this work, we address the integration of robust process and control design from a different perspective with optimization based *Constructive Nonlinear Dynamics* (CNLD). CNLD has originally been developed by the authors for the robust design of nonlinear process systems for which stability and feasibility in the presence of parametric uncertainty must be guaranteed (Mönnigmann and Marquardt, 2002). With some extensions, however, this method has also successfully been applied to the robust design of closed-loop systems (Mönnigmann and Marquardt, 2005). The method is based on imposing additional constraints on the system to guarantee a specified distance from critical boundaries in the space of

uncertain parameters. These boundaries separate those designs in the parameter space that exhibit desired properties from those which do not satisfy the desired properties. The general concept of critical boundaries allows to consider robust stability, feasibility, as well as robust performance of closed loop systems. One drawback of this versatile method so far, however, is the limitation to steady states and quasi-statically varying parameters (Mönnigmann and Marquardt, 2005). This is quite a severe restriction in a closed-loop control context as disturbances are generally fast compared to the system dynamics. In this paper an extension of CNLD is discussed to incorporate fast disturbances.

2. CRITICAL MANIFOLDS

Assume that a process model can be written as a system of nonlinear ordinary differential equations,

$$\dot{x} = f(x, p, d(\alpha, t)), \quad x(t_0) = x_0, \qquad (1)$$

with states $x \in \mathbb{R}^{n_x}$, initial conditions $x_0 \in \mathbb{R}^{n_x}$, constant process parameters $p \in \mathbb{R}^{n_p}$, which are known or can be set to a specified value, and time-varying disturbances $d \in \mathbb{R}^{n_d}$ parameterized by a set of uncertain parameters $\alpha \in \mathbb{R}^{n_\alpha}$. The right hand side, f, maps from $\mathbb{R}^{1+n_x+n_p+n_\alpha} \rightarrow \mathbb{R}^{n_x}$.

In the framework of CNLD, the structure of the disturbances has to be known except for the exact values of the uncertain parameters α. We assume that all α vary around a nominal value $\alpha^{(0)}$ by the uncertainty $\Delta\alpha$ according to

$$\alpha \in [\alpha^{(0)} - \Delta\alpha, \alpha^{(0)} + \Delta\alpha]. \qquad (2)$$

A simple example of a disturbance $d(\alpha, t)$ is a step disturbance triggered at t_0,

$$d(\alpha, t) = \begin{cases} 0, & t \le t_0 \\ \alpha, & t > t_0 \end{cases}, \qquad (3)$$

with α parameterizing the height of the disturbance. In the following we will replace disturbances $d(\alpha, t)$ by their parameterization t and α.

The system class (1) includes open-loop systems as well as closed-loop systems with specified control structure. In the latter case, system and control parameters are concatenated together in the parameter vector p. The flow of the nonlinear system (1) is given by

$$x = \chi(x_0, p, \alpha, t), \qquad (4)$$
$$\chi(x_0, p, \alpha, t_0) = x_0.$$

For nonlinear systems, the flow χ is generally not available in an analytical form but has to be evaluated by numerical integration. Let

$$0 < h(x, p, \alpha, t), \quad h \in \mathbb{R}, \quad t \in [t_0, t^e] \quad (5)$$

denote some time-varying bound on the trajectories of the process model which must not be violated at any time $t < t^e$. In the simplest case

$h = x_{1b} - x_1$ represents a constant upper bound for one of the state variables. Then the bound h is a straight line in the (x_1, t)-plane, which unfolds into a hyperplane in the space (x, α, t) of states, parameters, and time as shown in Fig. 1 (left).

Given the constraint (5), we can define two different kinds of critical manifolds. The first one is characterized by the set of trajectories which tangentially touch the hypersurface spanned by (5). The second one is defined by the set of trajectories where the constraint exactly holds at a specified final time t^e. The first type of points is closely related to the phenomena of grazing bifurcation of hybrid systems (Nordmark, 1991) where hitting the boundary h triggers a discrete event, e. g. the impact of a periodically forced oscillator on a solid wall. The grazing point corresponds to the trajectory where the system hits the boundary with zero velocity. Donde and Hiskens (2004) use manifolds of grazing bifurcations to calculate the closest grazing bifurcation from a nominal trajectory of a hybrid system. In this paper, however, boundaries (5) do not trigger a discrete event but are specified for safety reasons or product specifications.

2.1 Critical manifold of grazing points

Consider a realization x^* of the flow $\chi(x_0, p, \alpha, t)$ at t^* satisfying the constraint (5):

$$x^* - \chi(x_0, p, \alpha, t^*) = 0, \qquad (6)$$
$$h(x^*, p, \alpha, t^*) = 0.$$

Eq. (6) defines the time t^* and states x^* at which the trajectory corresponding to x_0, p, and α crosses the constraint (5). Assume that the system is subject to a step disturbance at t_0 with magnitude α_1. As can be inferred from Fig. 1 (left) a curve of points satisfying (6) unfolds in the (t, α_1)-plane by continuously varying α_1.
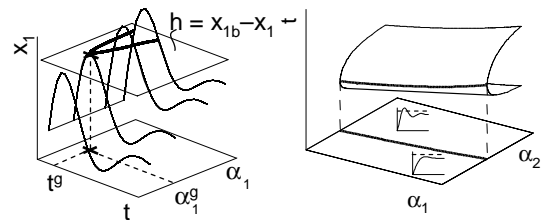

Fig. 1. Left: trajectories for different values of α_1 and curve (thick line) connecting points where trajectories cross the constraint $h = 0$. The grazing point is marked by $\times$. Right: manifold of grazing points. Trajectory sketches show on which side specified boundary $h = 0$ is not crossed.

The point (t^g, α_1^g) in Fig. 1 (left) marks the grazing point at which a trajectory touches tangentially the surface of the constraint. The tangent space of the hypersurface defined by constraint

(5) in the space (x, t), is spanned by the vector $[v^T, \tilde{v}]^T$ with $v \in \mathbb{R}^{n_x}$ and $\tilde{v} \in \mathbb{R}$ satisfying

$$\left[h_x^T, h_t \right] \begin{bmatrix} v \\ \tilde{v} \end{bmatrix} = 0,$$
$$v^T v + \tilde{v}^2 \neq 0. \tag{7}$$

h_x and h_t are the partial derivatives of the constraint h with respect to the state variables and time, respectively. At (x^g, t^g) the tangent space of the trajectory spanned by $[\dot{\chi}(x_0, p, \alpha, t)^T, 1]^T$ must satisfy (7). The deriviative of the flow with respect to time $\dot{\chi}$ is the right hand side f of the nonlinear system (1). The augmented system $M^{(g)}$ for a grazing point can therefore be written as

$$M^{(g)} = \begin{pmatrix} h(x, p, \alpha, t) \\ h_x f(x, p, \alpha, t) + h_t \end{pmatrix} = 0, \tag{8}$$

with the flow $x = \chi$ as defined in (4). These two equations determine the time t^g, and one parameter α_1^g at which the grazing point occurs.

Assume that there is a second disturbance at t_0 with magnitude α_2. The grazing point then unfolds to a curve (and the curve of crossing points into a two dimensional surface) in the three dimensional space (t, α_1, α_2) as shown in Fig. 1 (right). The curve of grazing points divides the parameter space into system designs with qualitative different behavior with respect to the constraint (5). In Fig. 1 (right) trajectories located on one side of this curve will not cross the constraint $h = 0$ for all times t, while transients of the system located on the other side of the critical manifold will always cross the boundary at some point after the step disturbances.

Note, that more than one critical manifold may exist for a constraint (5) in general if the trajectory touches or crosses the boundary several times. The region in the parameter space where the constraint is not violated is then the intersection of the regions devised by all critical manifolds.

2.2 Critical manifolds of endpoints

A second type of critical manifold can be defined for a bound on a trajectory by specifying a final time t^e at which the constraint must be exactly fulfilled as shown in Fig. 2 (left). Responses of system (1) after a step disturbance, parameterized by α_1 are shown together with the curve where the constraint h is crossed.

The trajectory with disturbance parameter $\alpha_1 = \alpha_1^e$ crosses the boundary at the specified time t^e. The augmented system defining the endpoint condition is given by

$$M^{(e)} = \begin{pmatrix} h(x, p, \alpha, t) \\ t - t^e \end{pmatrix} = 0. \tag{9}$$

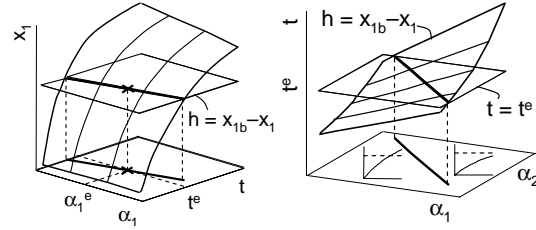These two equations determine the time t^e, and one parameter α_1^e.

Fig. 2. Left: trajectories for different values of disturbance parameter α_1 and curve (thick line) connecting points where trajectories cross the boundary $h = 0$. Critical point at t^e, α_1^e is marked by $\times$. Right: manifold of trajectories which fulfill constraint $h = 0$ at t^e after step disturbances of magnitude α_1 and α_2. Sketches of trajectories show in which region $h = 0$ is crossed or not.

By taking into account a second disturbance parameterized by α_2, the critical crossing point unfolds into a curve in the space (t, α_1, α_2) as shown in Fig. 2 (right). This curve separates a region in the parameter space (α_1, α_2) where the boundary is not touched or crossed until the specified time t^e is reached from a region where the constraint is always violated for $t < t^e$. This type of critical manifold is particularly useful for bounds on strictly monotonously increasing states or outputs where grazing points cannot occur.

3. NORMAL VECTORS ON CRITICAL MANIFOLDS

The basic idea of CNLD (Mönnigmann and Marquardt, 2002) is to utilize critical manifolds as defined in the previous section for the robust design of nonlinear systems. The approach enforces a lower bound on the parametric distance between a nominal operating point $\alpha^{(0)}$ and the nearest point $\alpha^{(c)}$ on the critical boundary. This lower bound ensures that the complete range of uncertain parameters is at a safe distance from the critical boundary as will be shown below.

The scaling of the parameters $\alpha_i \rightarrow \alpha_i / \Delta \alpha_i$, $\alpha_i^{(0)} \rightarrow \alpha_i^{(0)} / \Delta \alpha_i$ gives the dimensionless parameters

$$\alpha_i \in \left[\alpha_i^{(0)} - 1, \alpha_i^{(0)} + 1 \right]. \tag{10}$$

In this case the minimal distance is equal to the radius $\sqrt{n_\alpha}$ of the n_α-dimensional ball enclosing the n_α-dimensional cube of sidelength 2 defined by (10). In Fig. 3, a robust operating point is shown for $n_\alpha = 2$. The shortest distance between $\alpha^{(0)}$ and $\alpha^{(c)}$ occurs along the direction of the normal vector r to the critical manifold (Dobson, 1993). The minimal back off constraints can be stated as

$$\alpha^{(0)} = \alpha^{(c)} + l \frac{r}{\|r\|},$$
$$l \geq \sqrt{n_\alpha}. \tag{11}$$

The normal vector of critical manifolds can be calculated from the defining augmented systems
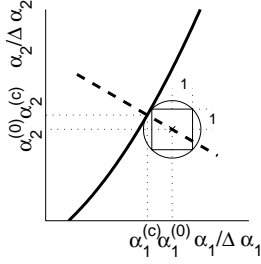
Fig. 3. Robust operating point $\alpha^{(0)}$ with critical manifold (thick line) and normal vector direction r (dashed thick line).

(8) and (9) following the scheme of derivation developed by Mönnigmann and Marquardt (2002). As parameters p and initial conditions x_0 are known, and because the states x are defined by the flow (4), the remaining variables are time t and uncertain parameters α. The normal space of the hypersurface defined by an augmented system $M^{(c)}$, $c \in \{g, e\}$ in the (t, α)-space is spanned by the Jacobian matrix of the partial derivatives $\nabla M^{(c)}$. The normal space of the augmented systems (8) and (9) is a $(n_\alpha + 1) \times (n_\alpha + 1)$ matrix

$$B = \begin{bmatrix} \nabla_t M_1^{(c)} & \nabla_t M_2^{(c)} \\ \nabla_\alpha M_1^{(c)} & \nabla_\alpha M_2^{(c)} \end{bmatrix}, \ c \in \{g, e\}. \quad (12)$$

For the augmented system of the grazing point (8), the entries of B are defined by

$$\nabla_t M_1^{(g)} = h_x f + h_t,$$
$$\nabla_t M_2^{(g)} = h_{xx} f f + h_x f_x f + h_x f_t + 2 h_{xt} f + h_{tt},$$
$$\nabla_\alpha M_1^{(g)} = h_x \chi_\alpha + h_\alpha,$$
$$\nabla_\alpha M_2^{(g)} = h_{xx} f \chi_\alpha + h_{x\alpha} f + h_x f_\alpha + h_x f_x \chi_\alpha +$$
$$h_{tx} \chi_\alpha + h_{t\alpha}.$$

The entries of B for the endpoint system (9) are

$$\nabla_t M_1^{(e)} = h_x f + h_t,$$
$$\nabla_t M_2^{(e)} = 1,$$
$$\nabla_\alpha M_1^{(e)} = h_x \chi_\alpha + h_\alpha,$$
$$\nabla_\alpha M_2^{(e)} = 0.$$

Note that the gradients include sensitivities χ_α of the flow with respect to the uncertain parameters α. Sensitivity equations are obtained by differentiating the dynamic system (1) with respect to α

$$\dot{\chi}_\alpha = f_x \chi_\alpha + f_\alpha.$$

A number of numerical integrators supports efficient evaluation of the sensitivity equations (e. g. Schlegel *et al.* (2004)).

The minimal distance in the space of the uncertain parameters α is in the direction of a vector $r \in \mathbb{R}^{n_\alpha}$ in the normal space (12) which has no contribution along the variable t. This vector is obtained by choosing an appropriate vector $\kappa \in \mathbb{R}^2$ such that

$$B\kappa = \begin{bmatrix} 0 \\ r \end{bmatrix} \in \mathbb{R}^{n_\alpha + 1}. \quad (13)$$

Together with the condition $\kappa^T z - 1 = 0$ with $z \in \mathbb{R}^2$ not normal to κ the two entries of κ are defined by the equations

$$\begin{bmatrix} \nabla_t M_1^{(c)} & \nabla_t M_2^{(c)} \end{bmatrix} \kappa = 0, \\ \kappa^T z - 1 = 0. \quad , c \in g, e \quad (14)$$

For the grazing point, i.e. $c = g$, this system of equations is solved by choosing $\kappa = [1, 0]^T$ and $z = \kappa$. The trailing n_α elements of (13) then give the n_α equations defining the normal vector r. The normal vector r can be calculated by combining the system of the normal vector equations with the augmented system defining the critical manifold (8) to result in

$$G^{(g)} = \begin{pmatrix} h(x, p, \alpha, t) \\ h_x f + h_t \\ h_x \chi_\alpha + h_\alpha - r \end{pmatrix} = 0. \quad (15)$$

For the endpoint constraint the system of equations (14) is solved by choosing $\kappa = [1, -(h_x f + h_t)]$ and $z = [1, 0]$. The augmented system of equations defining the normal vector direction for the endpoint constraint (9) then reads

$$G^{(e)} = \begin{pmatrix} h(x, p, \alpha, t) \\ t - t^e \\ h_x \chi_\alpha + h_\alpha - r \end{pmatrix} = 0. \quad (16)$$

The task of finding a system and control design minimizing an objective ϕ and guaranteeing that specified constraints (5) are never violated despite disturbances is addressed by solving the following constrained nonlinear program (NLP)

$$\min \phi(x^{(0)}, p^{(0)}, \alpha^{(0)}, t^{(0)}) \quad (17a)$$

$$\text{s. t. } x^{(0)} = \chi(x_0^{(0)}, p^{(0)}, \alpha^{(0)}, t^{(0)}),$$
$$0 < h^{(i)}(x^{(0)}, p^{(0)}, \alpha^{(0)}, t^{(0)}), \quad (17b)$$

$$x^{(i,j)} = \chi(x_0^{(0)}, p^{(0)}, \alpha^{(i,j)}, t^{(i,j)}),$$
$$0 = G^{(c,i,j)}(p^{(0)}, \alpha^{(i,j)}, t^{(i,j)}, r^{(i,j)}), \quad (17c)$$

$$0 = \alpha^{(i,j)} - \alpha^{(0)} + l^{(i,j)} \frac{r^{(i,j)}}{\|r^{(i,j)}\|}, \quad (17d)$$
$$0 \le l^{(i,j)} - \sqrt{n_\alpha}.$$

Eqs. (17b) define the states $x^{(0)}$ and constraints of the nominal system with upper index $i = 1 \ldots I$ enumerating the constraints. Eqs. (17c) define the states and augmented normal vector systems of the critical points. The superscript c denotes the type of critical manifold (grazing point or endpoint) and the index $j = 1 \ldots J_i$ enumerates the nearest critical manifolds for constraint i. Eqs. (17d) enforce the minimal back off between the nominal point and the critical manifold (i, j). The degrees of freedom of the NLP (17) are $p^{(0)}$, $\alpha^{(0)}$, $x_0^{(0)}$, $t^{(i,j)}$, $\alpha^{(i,j)}$, $r^{(i,j)}$, and $l^{(i,j)}$.

Note that the location of the critical manifolds corresponding to endpoints and grazing points are not known beforehand. Therefore the algorithm of Mönnigmann and Marquardt (2005) has to be employed where critical manifolds are detected as the optimization proceeds. If none of the determining critical manifolds is known a priori, optimization has to start without any robustness constraints (17c)-(17d). Detection of unknown critical points is implemented by numerical integration of system (1). The detection of critical points must therefore be realized on a finite time horizon with the length of the time horizon being a degree of freedom. Specification of the horizon length is a compromise between computational costs on the one hand and the risk of missing constraint violations after the time horizon on the other hand. Minimal distance constraints for the new detected manifolds are added to (17). By repeatedly solving the optimization problem and monitoring for new critical points, the set of known critical manifolds can be built up iteratively. If no further critical manifolds are detected along the optimization path, the robustness region has to be examined for critical manifolds which were not crossed by the nominal operating point during optimization, but which nevertheless might exist inside the robustness region. In this work this test is employed on a grid of points of the uncertainty region, e. g., on the corner or center points of the hypercube (2). A rigorous search for critical points within the uncertainty region can be implemented with interval arithmetics (Mönnigmann and Marquardt, 2005). Such a rigorous search is, however, computationally expensive and therefore only feasible for problems with a few uncertain parameters. If the tests reveal no further critical manifolds, an optimal operating point that is robust with respect to the specified parametric uncertainty is found and the algorithm terminates.

4. ILLUSTRATIVE CASE STUDY

Consider a continuous fermenter model with three nonlinear ODEs (c. f. Henson and Seborg (1992) for details on the model):

$$
\begin{aligned}
\dot{X} &= -DX + \mu X, \\
\dot{S} &= D(S_f - S) - \frac{\mu}{Y_{X/S}} X, \\
\dot{P} &= -DP + (\alpha\mu + \beta)X.
\end{aligned}
\tag{18}
$$

Here X, S, and P denote the three states biomass, substrate, and product concentration, μ is the growth rate:

$$
\mu = \frac{\mu_m \left(1 - \frac{P}{P_m}\right) S}{K_m + S + \frac{S^2}{K_i}}.
$$

The dilution rate D is the manipulated variable and the biomass concentration X the variable to be controlled with a PI controller

$$
D = D_0 + K_c \left(X_{\mathrm{sp}} - X + \frac{1}{\tau_i} \int_0^t (X_{\mathrm{sp}} - X)d\tau \right),
$$

with tuning parameters K_c and τ_i. The parameter values of the model are summarized in Table 1. According to Henson and Seborg (1992) the yield

Table 1. Parameter values

Parameter	Value	Parameter	Value
$Y_{X/S}^{(0)}$	0.4	$\mu_m^{(0)}$	$0.48\,\frac{1}{\mathrm{h}}$
α	2.2	β	$0.2\,\frac{1}{\mathrm{h}}$
P_m	$50\,\frac{\mathrm{g}}{\mathrm{L}}$	K_m	$1.2\,\frac{\mathrm{g}}{\mathrm{L}}$
K_i	$22\,\frac{\mathrm{g}}{\mathrm{L}}$	S_f	$20\,\frac{\mathrm{g}}{\mathrm{L}}$

$Y_{X/S}$ and the maximum specific growth rate μ_m may exhibit significant uncertainty. We assume therefore that both are subject to disturbances for $t > t_0$:

$$
\begin{aligned}
Y_{X/S} &= Y_{X/S}^{(0)} + \tilde{Y}_{X/S}, \\
\tilde{Y}_{X/S} &= \begin{cases} 0, & t \le t_0, \\ \Delta Y_{X/S}\left(1 - \exp\left((t - t_0)/\tau\right)\right), & t > t_0, \end{cases} \\
\mu_m &= \mu_m^{(0)} + \tilde{\mu}_m, \\
\tilde{\mu}_m &= \begin{cases} 0, & t \le t_0, \\ \Delta\mu_m \sin(\omega(t - t_0)), & t > t_0. \end{cases}
\end{aligned}
$$

The disturbance $\tilde{Y}_{X/S}$ is parameterized by the magnitude $\Delta Y_{X/S} \in [-0.05, 0.05]$ and the time constant set to $\tau = 2\,\mathrm{h}$. The sinusoidal disturbance $\tilde{\mu}_m$ is parameterized by the amplitude $\Delta\mu_m \in [-0.05, 0.05]$ and the frequency set to $\omega = 1\,\mathrm{h}^{-1}$.

We want to find an optimal operating point which minimizes the economic objective $\phi = -(10P - S_f)D$ for the undisturbed nominal case and a controller design that guarantees that the following constraints hold for all time even in the presence of disturbances $\tilde{\mu}_m$ and $\tilde{Y}_{X/S}$:

$$
\begin{aligned}
0 &< h_1 = PD - 3.0\,\left[\mathrm{g}\,(\mathrm{Lh})^{-1}\right], \\
0 &< h_2 = 6.5\,\left[\mathrm{g}\,\mathrm{L}^{-1}\right] - S, \\
0 &< h_3 = 1.25\,\left[\mathrm{hg}^2\mathrm{L}^{-2}\right] - \int_0^t (X_{\mathrm{sp}} - X)^2 d\tau.
\end{aligned}
\tag{19}
$$

The first two constraints guarantee a minimal reactor yield and an upper bound on the substrate concentration in the product stream. The upper bound on the integrated squared tracking error (ISE) guarantees a minimal performance of the closed loop. Constraints h_1 and h_2 are implemented as minimal back off from critical manifolds of grazing points. For the ISE criterion, however, a grazing point cannot occur as the ISE increases monotonically and complete supression of the sinusoidal disturbance cannot be expected. Therefore, a minimal distance constraint to an endpoint condition (16) is established. The end time is set to $t^e = 200\,\mathrm{h}$ which is roughly 30 times the time constant of the open loop process. The length of the time horizon for the detection of critical points is chosen accordingly to 200 h.

For the nominal operating point steady state constraints $0 = f^{(0)}$ are employed replacing the flow in (17b). For the nominal point the ISE constraint h_3 of (19) is therefore automatically fulfilled. The initial values of the critical trajectories (i, j) are set to the nominal steady states $x_0^{(i,j)} = x^{(0)}$. In this scenario the fermentor runs at its steady state operating point $x^{(0)}$ with disturbances $\tilde{Y}_{X/S}$ and $\tilde{\mu}_m$ starting at t_0. The control design and operating point obtained by solving the NLP (17) guarantees that all possible trajectories resulting from these disturbances starting from initial conditions $x_0^{(i,j)} = x^{(0)}$ do not cross the specified constraints (19). Free optimization variables are the tuning parameters K_c, τ_i, the nominal dilution rate D_0, the set point of the biomass concentration X_{sp}, the substrate feed concentration S_f and the steady state variables of the nominal system $X^{(0)}, S^{(0)}, P^{(0)}$.
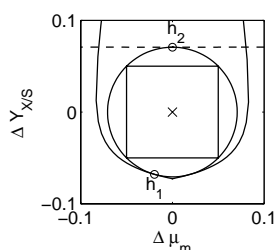

Fig. 4. Robustness ellipse in the plane of the uncertain disturbance parameters. Two constraints h_1 (continuous line) and h_2 (dashed line) are active for the robustly optimal process and control design.

Optimization starts without robustness constraints. Unknown critical manifolds are detected by numerical integration and repeated optimization steps. Each detected critical manifold adds a normal vector constraint with four new variables $t^{(i,j)}$, $l^{(i,j)}$, $\Delta\mu_m^{(i,j)}$, $\Delta Y_{X/S}^{(i,j)}$ to the NLP. At the robust optimum, two minimal distance constraints are active for bounds h_1 and h_2 with $l^{(i,j)} = \sqrt{2}$ as shown in Fig. 4. This guarantees that the specified bounds hold despite the disturbances. The resulting design is summarized in Table 2.

Table 2. Optimal operating point

Parameter	Value	Parameter	Value
S_f	$17.82 \frac{\mathrm{g}}{\mathrm{L}}$	D_0	$0.218 \frac{1}{\mathrm{h}}$
$X^{(0)}$	$5.33 \frac{\mathrm{g}}{\mathrm{L}}$	$S^{(0)}$	$4.50 \frac{\mathrm{g}}{\mathrm{L}}$
$P^{(0)}$	$16.61 \frac{\mathrm{g}}{\mathrm{L}}$	K_c	-7.19
τ_i	$0.1098\mathrm{h}$		

5. CONCLUSIONS

In this paper an extension to the method of Constructive Nonlinear Dynamics has been presented. This approach enables the robust optimization of nonlinear systems such that specified dynamics or feasibility can be guaranteed even in the presence of uncertainty. Here, the idea of backing off from critical manifolds is extended from steady state design to constraints on trajectories of nonlinear systems. Minimal distance constraints based on normal vector directions to critical manifolds of grazing points and endpoints guarantee that bounds on states and inputs hold for all times even in the presence of fast disturbances. For closed loop systems, this method can be used for the simultaneous system and control design. The case study presented in this paper shows the feasibility of the approach for robust control and process design in the presence of fast disturbances. In this study only simple disturbance signals were considered. In the future, therefore the influence of more complex disturbances will be investigated.

REFERENCES

Dobson, I. (1993). Computing a closest bifurcation instability in multidimensional parameter space. *J. Nonlinear Sc.* **3**, 307–327.

Donde, V. and I.A. Hiskens (2004). Guaranteeing performance in nonlinear non-smooth power systems. In: *Preprints Volume 1-3 of NOLCOS 2004, Stuttgart.* pp. 1331–1336.

El-Farra, N.H. and P.D. Christofides (2001). Integrating robustness and constraints in control of nonlinear processes. *Chem. Eng. Sci.* **56**, 1841–1868.

Henson, M.A. and D.E. Seborg (1992). Nonlinear control strategies for continuous fermenters. *Chem. Eng. Sci.* **47**, 821–835.

Kurtz, M.J. and M.A. Henson (1997). Input-output linearizing control of constrained nonlinear processes. *J. Process Contr.* **7**, 3–17.

Mayne, D.Q. J.B. Rawlings, C.V. Rao and P.O.M. Scokaert (2000). Constrained model predictive control: Stability and optimality. *Automatica* **36**, 789–814.

Mönnigmann, M. and W. Marquardt (2002). Normal vectors on manifolds of critical points for parametric robustness of equilibrium solutions of ODE systems. *J. Nonlinear Sc.* **12**, 85–112.

Mönnigmann, M. and W. Marquardt (2005). Steady state process optimization with guaranteed robust stability and flexibility: Application to HDA reaction section. *Ind. Eng. Chem. Res.* **44**, 2737–2753.

Nordmark, A.P. (1991). Nonperiodic motion caused by grazing-incidence in an impact oscillator. *J. Sound Vib.* **145**, 279–297.

Schlegel, M., W. Marquardt, R. Ehrig and U. Nowak (2004). Sensitivity analysis of linearly-implicit differential-algebraic systems by one-step extrapolation. *Appl. Num. Math.* **48**(1), 83–102.